Dynamical Behavior of Semidilute Polymer Solutions in a Θ Solvent: Quasi-Elastic Light Scattering Experiments

M. Adam* and M. Delsanti

Service de Physique du Solide et de Rêsonance Magnêtique, CEN-Saclay, 91191 Gif-sur-Yvette, Cedex, France. *Received July 7, 1984*

ABSTRACT: We report experiments performed with a heterodyne spectrometer at the Θ temperature in the polystyrene–cyclohexane system. Two dynamical regimes are observed: a liquid regime and a gel regime. In the liquid regime, where the semidilute solution behaves like a viscous fluid, the time dependence of the dynamical structure factor is well described by a single-exponential function. The macroscopic mutual diffusion coefficient is related to the motion of the solvent through the polymer. In the gel regime, where the solution behaves like an elastic gel, the dynamical structure factor is multiexponential (>2). The two processes that control the relaxation of concentration fluçtuations are the motion of the solvent through the transient gel and the structural relaxation of the transient gel. When the temperature is increased above the Θ temperature, the nonexponentiality of the dynamical structure factor in the gel regime disappears and we recover an exponential function as in good solvent solutions (polystyrene–benzene). In a Θ solvent, both liquid and gel regimes are observed because dynamical properties are governed by two different lengths as was shown previously by viscoelastic measurements.

Introduction

The static and dynamic properties of semidilute polystyrene solutions have been intensively studied by several kinds of experiments. We recall the main results.

In a Θ solvent as well as in a good solvent, light and neutron scattering[1–5] and osmotic pressure[6] measurement show that the correlation length ξ of the concentration fluctuation correlation function and the osmotic pressure Π are independent of the molecular weight of the polymer.

The sedimentation coefficient[7,8] measured in a semidilute Θ solution shows that the hydrodynamic screening length ξ_H is proportional to ξ.

Shear viscoelastic measurements[9–10] have shown clearly that the semidilute solution behaves like an elastic gel at short time and like a viscous fluid at long time. The characteristic time T_R which separates elastic and viscous regimes is related to the lifetime of contact points between polymers, and it depends strongly on the molecular weight of the polymer. The influence of the contact points on the motion of a "labeled" chain leads to a self-diffusion coefficient which strongly depends on the molecular weight, as has been shown by forced Rayleigh[11,12] and nuclear magnetic resonance.[13,14]

The time behavior of the concentration fluctuation correlation function was first determined in a semidilute polymer solution in a good solvent (polystyrene–benzene).[15] At a time scale where the semidilute solution behaves like an elastic gel ($t < T_R$), the time dependence of the correlation function was well described by a single-exponential function.[15,17] The mutual diffusion coefficient measured by quasi-elastic light scattering (QELS)[15,16] at $t < T_R$ is slightly larger (10%) than that measured at $t > T_R$ using classical gradient diffusion.[18,19] These mutual diffusion coefficients have the same concentration dependence and are molecular weight independent.

Here we present QELS experiments performed for a wide range of molecular weights and concentrations. First of all, we will present a theoretical description of the dynamics of semidilute Θ solutions. The main idea is due to Brochard and de Gennes,[22,23] where the following hypothesis was given: the elastic modulus was considered to be much larger than the osmotic bulk modulus. Since experimental results[10] lead to moduli of the same order of magnitude, we have released the hypothesis and obtained theoretical results quantitatively different from those obtained in ref 22 and 23.

I. Theoretical Description

A polymer solution is semidilute if the monomer concentration c is smaller than the solvent concentration but higher than the overlap concentration:

$$c^* = Nm/R_g^3 \tag{1}$$

m is the weight of the monomer and R_g is the radius of gyration of the polymer having a degree of polymerization N.

The dynamical behavior of semidilute polymer solutions has been discussed by de Gennes and Brochard.[20–24] The pair correlation function between the monomer has the screened form[24]

$$g(r) = \frac{k_B T_e}{4\pi\xi^2(\partial\Pi/\partial c)} \frac{e^{-r/\xi}}{r} \tag{2}$$

where k_B and T_e are respectively the Boltzmann constant and the absolute temperature and ξ is the correlation length, which is independent of the degree of polymerization. The polymer solution is considered as a transient gel[20,21] with a mesh size ξ_2 equal to the mean distance between two successive binary contact points. In a good solvent ξ and ξ_2 are proportional.[21] Since only one characteristic length exists in the system, all the dynamic and static properties have one reduced variable: c/c^*. This is in agreement with experimental results (see for example ref 6 and 9).

In a Θ solvent, where the binary thermodynamic interactions vanish, ξ_2 is smaller and no longer proportional to ξ[22]

$$\xi \sim \xi_2^2 \sim c^{-1}N^0 \qquad \text{(ref 25)} \tag{3}$$

but the hydrodynamic screening length ξ_H is proportional to ξ[22]

$$\xi_H \simeq \xi \tag{4}$$

Let us focus on the macroscopic longitudinal displacement $u(q,\omega)$ of the polymer at the frequency ω and at the wave vector q such that $q\xi \ll 1$. $u(q,\omega)$ is governed by the equation of motion[23] which expresses a balance between the viscous and the restoring force. The latter is composed of the elastic force and the osmotic force. The viscous force is due to the friction between the polymer and the solvent. The equation of motion is

$$i\omega cu/\mu + Kq^2u + M(\omega)q^2u = 0 \tag{5}$$

0024-9297/85/2218-1760$01.50/0

The effective mobility μ per monomer is

$$\mu = \frac{c\xi^3}{6\pi\eta_0\xi_H} \sim c^{-1}N^0 \quad (6)$$

where η_0 is the solvent viscosity. The osmotic bulk modulus K is related to the osmotic pressure Π and scales with the concentration as

$$K = c(\partial\Pi/\partial c) \simeq k_BT_e/\xi^3 \sim c^3N^0 \quad (7)$$

The osmotic force Kq^2u tends to make the monomer concentration uniform. The longitudinal elastic modulus, M, of the transient gel is frequency dependent

$$M(\omega) = M_g - M_g/(1 + i\omega\tau_R) \quad (8)$$

The longitudinal relaxation time τ_R, related to the lifetime of the transient gel, is strongly dependent on the degree of polymerization: $\tau_R \sim N^3$ (reptation model[20,21]). M_g, the elastic modulus of the transient gel, is proportional to the density of binary contact points c/p, where p is the number of monomers between two successive binary contact points: $M_g \simeq k_BT_ec/p$. In a Θ solvent the polymer chain is Gaussian at any scale, and the mean quadratic distance ξ_2^2 is proportional to p. So we have

$$M_g \sim c/\xi_2^2 \sim c^2N^0 \quad (9)$$

M_g is not proportional to K.

The dispersion relation derived from the equation of motion (5) is

$$\Gamma(q) = (\mu/c)(K + M(\omega))q^2 \quad (10)$$

At low frequency ($\omega\tau_R \ll 1$), the polymer system behaves like a liquid ($M = 0$) and the characteristic frequency $\Gamma(q)$ of the nonpropagating macroscopic displacement is

$$\Gamma(q) = (\mu/c)Kq^2 = D_cq^2 \quad (11)$$

At high frequency ($\omega\tau_R \gg 1$), the polymer system behaves like a gel ($M(\infty) = M_g$) and we have

$$\Gamma(q) = (\mu/c)(K + M_g)q^2 = D_gq^2 \quad (12)$$

At high and low frequency, the displacement is due to diffusion. Both the osmotic (D_c) and the gel (D_g) diffusion coefficients are molecular weight independent. Using the expressions of the effective mobility μ (eq 6) and of the osmotic bulk modulus K (eq 7), we obtain for the osmotic diffusion coefficient

$$D_c \simeq k_BT_e/6\pi\eta_0\xi_H \quad (13)$$

Since the hydrodynamic screening length ξ_H is proportional to ξ, D_c is proportional to the concentration. The relative difference between the gel diffusion coefficient and the osmotic diffusion coefficient is equal to the ratio of the longitudinal elastic modulus of the transient gel M_g to the bulk osmotic modulus K

$$D_g/D_c - 1 = M_g/K \quad (14)$$

Using the expressions of M_g (eq 9) and K (eq 7), we find that $D_g/D_c - 1$ is inversely proportional to the concentration.

So far we have discussed macroscopic displacement ($q\xi \ll 1$); let us now focus our attention on local displacement, i.e., displacement on a scale smaller than ξ ($q\xi \gg 1$). This regime has been analyzed by Brochard.[23] We will consider only the case $q\xi \gg 1$ but with $q\xi_2 \ll 1$, which is the case encountered experimentally for the range of concentration, molecular weight, and wave vector investigated. In this regime, M_g does not depend on q (because $q\xi_2 \ll 1$), but K and μ are q dependent (because $q\xi \gg 1$)

$$K(q) = K(1 + q^2\xi^2) \quad \text{(ref 2)} \quad (15)$$

$$\mu(q) = \mu F(q\xi) \quad (16)$$

$F(q\xi)$ is a scaling function of $q\xi$

$$F(q\xi) = 1 \quad \text{for } q\xi = 0$$

$$F(q\xi) \simeq 1/q\xi \quad \text{for } q\xi \gg 1$$

In the range $q\xi \approx 1$, the exact form of $F(q\xi)$ depends on the approximation used.[23,26]

The characteristic frequency of the displacement $\Gamma(q)$ is given by an expression similar to eq 12 where μ and K, instead of being macroscopic quantities, are replaced by eq 15, and 16. This leads to

$$\Gamma(q) = D_gq^2F(q\xi)\frac{M_g/K + 1 + q^2\xi^2}{M_g/K + 1} \quad (17)$$

In the asymptotic regime ($q\xi \gg 1$)

$$\Gamma(q) = D_gq^2 \times q\xi \quad \text{if } M_g/K = 0$$

$$\Gamma(q) = D_gq^2/q\xi \quad \text{if } M_g/K \gg q^2\xi^2 \quad (18)$$

Thus, depending on the relative magnitude of the longitudinal elastic modulus to the bulk osmotic modulus, one has either a q^3 or a q dependence of the characteristic frequency.

It is well-known that the light scattered by a polymer solution is sensitive to the qth Fourier component of the displacement and to its characteristic frequency. The aim of this work is to show that the three different behaviors of $\Gamma(q)$ are observable by choosing appropriate samples and transfer vectors. In section II we give the experimental procedure and in particular the experimental conditions, molecular weights, and transfer vectors available.

II. Experimental Procedure

1. Samples and Temperature Control. Polystyrene and cyclohexane (norma pur) were purchased from Toyo Soda and Prolabo, respectively. In order to avoid degradation or anomalous states, the solutions are never frozen.[27] The solutions are prepared directly into the unsealed light scattering cell without shaking and without filtration at room temperature (20 °C). The monomer concentration is determined by weighing. Then the samples are maintained in an oven at 50 °C for several months (at least 9 months). If any accidental demixing occurs, it is necessary to maintain the system several weeks at 50 °C in order to reobtain a homogeneous solution. The homogeneity is checked by measuring the viscosity at various locations of the cell with the magnetic sphere rheometer.[10,28] The evaporation of the solvent is controlled by weighing just after experiments are performed. We are confident in the homogeneity of the samples and in the fact that the light scattered by dust particles is negligible. Actually, the same samples were used for the intensity light scattering experiments:[4] the intensity scattered at zero momentum transfer for a given concentration was independent of the molecular weight; the correlation length of the concentration fluctuation correlation function agrees with neutron scattering experiments.[2]

In Table I we report the characteristics of the polymers: the molecular weights M_w and M_n, the concentration dependence of the longest shear viscoelastic relaxation time T_R, and the overlap concentration c^*. T_R is measured with the magnetic sphere rheometer,[28] which allows the shear stress relaxation, after cessation of a constant shear rate, to be determined. The overlap concentration is calculated with the definition of c^* given in eq 1 and the value of the radius of gyration, R_g, determined by intensity light scattering experiments.[29] We obtain

$$c^* \text{ (g/cm}^3\text{)} = 40/M_w^{1/2} \quad (19a)$$

It appears that this numerical value of c^* corresponds to the crossover between dilute and semidilute regimes for the osmotic

Table I
Sample Characteristics and Corresponding Symbols Used in the Figures

$M_w \times 10^{-6}$	M_w/M_n	10^2c^*, g/cm^3	symbol	T_R,[a] s
0.422	1.05	6.16	●, no pip	$8.7 \times 10^{-2}c^{2.8}$ (e)
1.26	1.05	3.56	×	$5.5c^{2.8}$ (e)
2.89	1.09	2.35	●, pip up	$1.3 \times 10^2c^{2.8}$ (e)
3.84	1.04	2.04	●, pip left	$3.29 \times 10^2c^{2.75}$
6.77	1.14	1.54	●, pip right	$3.30 \times 10^3c^{2.85}$
20.6		0.88	●, pip down	$1.95 \times 10^5c^{2.75}$

[a] The concentration dependence of the shear viscoelastic relaxation time T_R if given. ((e) Means that the law is obtained by extrapolation from the measurements performed with high molecular weights ($M_w \geq 3.84 \times 10^6$).)

compressibility.[4] In order to fulfil the criteria of the semidilute regime, the monomer concentration c of the samples is such that

$$c^* < c \lesssim 0.11 \text{ g/cm}^3 \quad \text{(ref 14)} \tag{19b}$$

The temperature Θ is chosen equal to 35 °C when the second virial coefficient of the osmotic pressure vanishes.[30]

For QELS measurements, the scattering cell with a square cross section is set in a thermally regulated copper jacket. The temperature, measured with a thermocouple in contact with the cell, is homogeneous and stable within the accuracy of the measurement (±0.04 °C).

2. Light Scattering Apparatus and Data Analysis. The monochromatic light source is provided by an argon laser (4880 Å) or a helium–neon laser (6328 Å). The light power (≲3 mW) and the convergence of the incident beam are such that there is no thermal lens effect and no multiple scattering. The spectrometer is a two-beam heterodyne light beating spectrometer; a complete description of the experimental setup can be found in ref 15. By means of a beam splitter 4% of the incident beam is used as a local oscillator, whose intensity and polarization are adjusted by means of two polarizers. In heterodyne detection the scattered electric field is mixed with the local oscillator on the photocathode of the photomultiplier. To switch from heterodyne to homodyne detection a screen is placed on the local oscillator beam. With this experimental setup the scattering angle available goes from 8° to 175° (in air). The momentum transfer range investigated is

$$1.4 \times 10^4 \leq q \leq 3.6 \times 10^5 \text{ cm}^{-1} \tag{20}$$

The autocorrelation function of the photopulses is realized by a 128-channel multibit correlator which is interfaced to a microcomputer.

In heterodyne detection, at a momentum transfer q, the autocorrelation of photopulses, $C(q,t)$, directly gives the time dependence $\tilde{S}(q,t)$ of the dynamical structure factor.[31]

$$C(q,t) \simeq I_0[2\alpha I_q \tilde{S}(q,t) + I_0] \quad \text{if } \alpha I_0 \gg I_q \tag{21}$$

I_0 is the intensity of the local oscillator that beats with the scattered light (I_q). α represents the efficiency of the coherent wave front matching ($0 \leq \alpha \leq 1$); when the matching is perfect, α is equal to 1. To experimentally check the heterodyne condition (eq 21), we verify that the ratio base line ($\sim I_0^2$) to signal ($\sim 2\alpha I_0 I_q$) is proportional to the intensity of the local oscillator.

In order to analyze the profile of $\tilde{S}(q,t)$, the following procedure is used. The measurement is done on a correlator time window T which goes from Δt to $T = n\Delta t$; Δt and n are the time per channel and the number of channels of the correlator, respectively ($\Delta t_{min} = 10^{-7}$ s and $T_{max} = n\Delta t \approx 10^2$ s). The resulting experimental function $C_T(q,t)$ is fitted to an exponential line shape with a base line by a least-squares procedure; we minimize the quantity

$$\sum_{i=1}^{n} \{C_T(q,i\Delta t) - B_T[R_T \exp(-i\Delta t/\tau_T) + 1]\}^2 \tag{22}$$

where $R_T B_T$, B_T, and τ_T are three adjustable parameters.

In order to estimate the precision on the decay time τ_T, we calculate the relative standard deviation from the error matrix[32]

$$V_T = \langle \delta_T^2 \rangle^{1/2}/\tau_T \sim \left(\frac{1}{n-3} \sum_{i=1}^{n} \epsilon_i^2 \right)^{1/2} \tag{23}$$

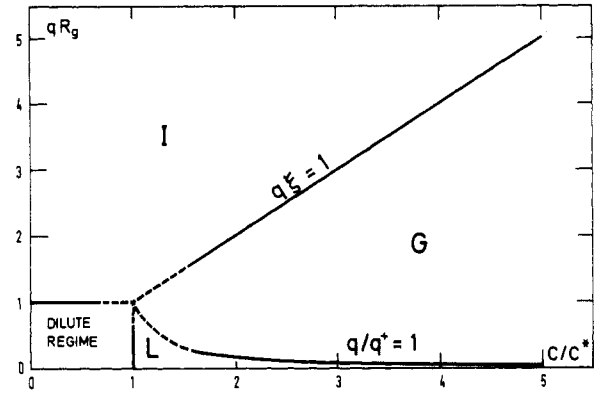

Figure 1. Different regimes investigated by QELS, schematically represented in the plane qR_g vs. c/c^*. The lines represent the crossover between different regimes. The lower line $q/q^\dagger = 1$ (see eq 27) represents the transition from the liquid (L) to the gel (G) regime. The upper line represents the transition from macroscopic to internal motion (I regime): $qR_g = 1$ and $q\xi = 1$ in the dilute and in semidilute regimes, respectively.

ϵ_i is the deviation of the ith experimental point from the corresponding calculated value.

In order to check if the exponential profile describes the observation, we calculate the quality factor[33]

$$Q_T = 1 - |\sum_{i=1}^{n-1} \epsilon_i \epsilon_{i+1}| / \sum_{i=1}^{n} \epsilon_i^2 \tag{24}$$

In ϵ_i there are two contributions, a statistic error ϕ_i and a systematic error δ_i. Q_T gives an evaluation of the contribution of the statistical and systematic errors to the total error. At first order we have

$$Q_T = \sum_i \phi_i^2 / \sum_i \epsilon_i^2 \tag{25a}$$

and

$$1 - Q_T = \sum_i \delta_i^2 / \sum_i \epsilon_i^2 \tag{25b}$$

At a given momentum transfer q, by varying the correlator time window T, we investigate the behaviors of the three parameters τ_T, V_T, and Q_T. The correlator time window T is varied either by a continuous increase or by an iterative procedure. In the latter method the initial measurement is done at T_1, which gives a decay time τ_{T_1}, the second measurement at $T_2 = 3\tau_{T_1}$, and the jth measurement at $T_j = 3\tau_{T_{j-1}}$. After a few iterations (≈2), this procedure reaches a time window and a decay time which are constant (within ±2%) only if the correlation function is a single exponential. This analysis is performed at different values of q in the whole range of q available (eq 20).

The comparison of the autocorrelation functions $C(q,t)$ obtained with heterodyne and the homodyne detection is useful in the characterization of the time dependence of the dynamical structure factor $\tilde{S}(q,t)$. This can be easily done with our experimental light scattering setup. On the other hand, heterodyne detection allows us to have a replica of $\tilde{S}(q,t)$, which is useful when the line shape is multiexponential.

Due to the complexity of the dynamics of semidilute Θ solutions, in section III we derive the forms of the dynamical structure factors expected in the three regions of Figure 1.

III. Dynamical Structure Factor

As in section I, we assume that the disentanglement of the chains can be described by a single relaxation time τ_R.

At a given momentum transfer q, the scattered light reflects the properties at a scale q^{-1}. If $q\xi \ll 1$ (and therefore $q\xi_2 \ll 1$), the polymer solution can be considered as homogeneous, and the dynamical structure factor reflects the macroscopic properties of the polymer solution. If $q\xi \gg 1$, the dynamical structure factor reflects the local properties inside ξ. The upper line in Figure 1, $q\xi = 1$, corresponds to the crossover between macroscopic and local properties.

Let us first consider the case $q\xi \ll 1$, which corresponds to the region G and L in Figure 1.

1. Macroscopic Regime ($q\xi \ll 1$). Using an approach similar to that used in ref 22 and 23 (see appendix), we find that the dynamical structure factor $S(q,t)$ is the sum of two exponential functions

$$S(q,t) = \frac{k_B T_e c^2}{K}\tilde{S}(q,t)$$

and

$$\tilde{S}(q,t) = A_S e^{-t/\tau_{Sg}} + A_L e^{-t/\tau_{Lg}} \tag{26a}$$

The relative amplitudes of the two components are linked to the decay times τ_S and τ_L

$$A_S = (\tau_R - \tau_S)/(\tau_L - \tau_S)$$

$$A_L = 1 - A_S = (\tau_L - \tau_R)/(\tau_L - \tau_S) \tag{26b}$$

The characteristic decay times have the following dependences:

$$1/\tau_L D_c q^2 = \frac{1}{2}\frac{D_g}{D_c}(q^{\dagger 2}/q^2 + 1) \times \left[1 - \left(1 - 4\frac{D_c q^2}{D_g q^{\dagger 2}(1 + q^2/q^{\dagger 2})^2}\right)^{1/2}\right]$$

$$\tau_S^{-1}/\tau_R^{-1} = \frac{1}{2}\left(1 + \frac{q^2}{q^{\dagger 2}}\right)\left[1 + \left(1 - 4\frac{D_c q^2}{D_g q^{\dagger 2}(1 + q^2/q^{\dagger 2})^2}\right)^{1/2}\right] \tag{26c}$$

where

$$q^\dagger = (1/\tau_R D_g)^{1/2} \tag{27}$$

and D_g and D_c are the gel and osmotic diffusion coefficient, respectively (eq 11 and 12).

At a given momentum transfer q, the time required by the polymer system to diffuse on a scale q^{-1} is $(D_g q^2)^{-1}$; at $q = q^\dagger$ this time is equal to τ_R. In Figure 1, $q/q^\dagger = 1$, which corresponds to the lower line, is calculated for 4×10^6 molecular weight, setting $M_g/K = 5 \times 10^{-2}/c$ in eq 12 (see eq 30 and 38) and assuming, following the reptation model, that

$$\tau_R = \frac{6\pi\eta_0 R_g^3}{k_B T_e}\left(\frac{c}{c^*}\right)^3$$

One must note that this line is molecular weight dependent in this representation. But, whatever the exact form of τ_R and M_g/K, the plane qR_g vs. c/c^* for $c/c^* > 1$ and $q\xi \ll 1$ is always divided into two regions

$q < q^\dagger$ liquid regime (L)

$q > q^\dagger$ gel regime (G)

$q^\dagger$ is a momentum transfer that separates the two dynamical behaviors, which will be analyzed successively.

a. Liquid Regime ($q \ll q^\dagger$, Region L in Figure 1). In this limit the expressions (26) of the decay times and the amplitudes reduce to

$$\tau_L \equiv \tau_{Lc} = 1/(D_c q^2)$$

$$\tau_S = \tau_R$$

$$A_L = 1$$

and

$$A_S = 0 \tag{28}$$

The time dependence of the dynamical structure factor is a single-exponential function because the amplitude of the first term in $\tilde{S}(q,t)$ (26a) vanishes

$$\tilde{S}(q,t) = e^{-t/\tau_{Lc}} \tag{29}$$

b. Gel-like Regime ($q \gg q^\dagger$, Region G in Figure 1). In this limit, the expressions (26) of the decay times and the amplitudes reduce to

$$\tau_L \equiv \tau_{Lg} = \tau_R D_g/D_c$$

$$\tau_S \equiv \tau_{Sg} = 1/(D_g q^2)$$

$$A_L/A_S = D_g/D_c - 1 = M_g/K \tag{30}$$

The time dependence of the dynamical structure is the sum of two exponential functions

$$\tilde{S}(q,t) = A_S e^{-t/\tau_{Sg}} + A_L e^{-t/\tau_{Lg}} \tag{31}$$

The first component is related to the diffuse displacement of the polymer at high frequency (eq 12). The slow component, which has a q-independent decay time, corresponds to a structural relaxation.

The fluctuation of the concentration induces a concentration gradient and an elastic stress. At short time, the concentration relaxes with a decay time $(D_g q^2)^{-1}$. During this time $(D_g q^2)^{-1} \ll \tau_R$, the polymer system can be considered as a permanent gel. At long times, the elastic stress relaxes via the longest viscoelastic relaxation time $(\tau_R D_g/D_c)$.

For $q\xi < 1$, the total intensity scattered is independent of $q/q^\dagger$ and proportional to the osmotic compressibility, it is thus molecular weight independent. On the other hand, for $q\xi > 1$, the intensity is q dependent. $q^\dagger$ is linked to a characteristic time and ξ is a characteristic length of the semidilute polymer solution.

2. Internal Motion Regime ($q\xi > 1$, Region I of Figure 1). We focus our attention on the fast relaxation process and on the condition $q\xi_2 < 1$, where ξ_2 is the mean distance between binary contact points.

Since the condition $q^\dagger < \xi^{-1}$ is always fulfilled, the semidilute solution can be considered to be a permanent gel. The inverse of the decay time of the fast component of the dynamical structure factor is equal to the characteristic frequency of the displacement discussed in section I (eq 17)

$$\tau_{Sg}^{-1} = D_g q^2 F(q\xi)\frac{M_g/K + 1 + q^2\xi^2}{M_g/K + 1} \tag{32}$$

If, as was predicted in section I, M_g and K do not have the same concentration dependence ($M_g/K \sim c^{-1}$; see eq 7 and 9), $q\xi$ is not a reduced variable of $\tau_{Sg}^{-1}/(D_g q^2)$. At a given value of $q\xi$, whatever the exact form of $F(q\xi)$ is, when the concentration is decreased, the ratio $1/\tau_{Sg} D_g q^2$ must decrease.

A given semidilute sample is characterized by two quantities: the correlation length ξ, which is only concentration dependent, and the transfer vector $q^\dagger$, which is concentration and molecular weight dependent.

The knowledge of the concentration and molecular weight of a sample allows us to locate the region in Figure 1 that will be investigated experimentally. The dynamical structure factor of a semidilute Θ solution must have, in the three regions of Figure 1, the following expected behavior:

Table II
Decay Times and Amplitudes of the Components of the Dynamical Structure Factor (See Figure 1)

regime	decay time τ_S	decay time τ_L	amplitude of component
liquid regime (L)		$\tau_{Lc} = 1/(D_c q^2)$	$A_L = 1$ $A_S = 0$
gel regime (G)	$\tau_{Sg} = 1/(D_g q^2)$	$\tau_{Lg} = D_g \tau_R / D_c$	$A_L/A_S = D_g/D_c - 1$
internal motions (I)	$\tau_{Sg} \sim q^x$, $1 \le x \le 3$		

$q\xi \ll 1$

$q < q^\dagger$ (*Liquid Regime, Region L of Figure 1*)

The profile of $\tilde{S}(q,t)$ is a single-exponential function with a decay time inversely proportional to the osmotic diffusion coefficient D_c (see eq 11).

$q > q^\dagger$ (*Gel Regime, Region G of Figure 1*)

$\tilde{S}(q,t)$ is a two-exponential function. The decay time of the fast component is inversely proportional to the gel diffusion coefficient D_g (see eq 12). The decay time of the slow component is independent of q and must be related to the viscoelastic relaxation time.

$q\xi \gg 1$ (*Region I of Figure 1*)

$\tilde{S}(q,t)$ has the same form as in the gel regime but the fast decay time is related to internal motions inside the correlation length. The study of these motions must allow us to point out the influence of two lengths in semidilute Θ solutions.

The main behaviors of $\tilde{S}(q,t)$ are summarized in Table II.

In the next section we present results obtained over a wide range of molecular weights, concentrations, and transfer vectors. The procedure used to analyze the experimental correlation function (Section II) presents the advantage that no a priori assumptions have to be done on the $\tilde{S}(q,t)$ profile.

IV. Experimental Results and Discussion

1. Macroscopic Liquid and Gel Regimes (Regions L and G of Figure 1). From neutron[2] and light scattering experiments,[4] the correlation length of the concentration fluctuations was determined to be

$$\xi \text{ (cm)} = 5.5 \times 10^{-8}/c \qquad (33)$$

In order to observe macroscopic quantities, the experimental condition is $q\xi < {}^1/_3$ or $q < 6 \times 10^{-6} c$ (for more details, see section IV.b).

a. Liquid Regime ($q < q^\dagger$, Region L of Figure 1). Here we present the results obtained from experiments done on samples having very small shear viscoelastic relaxation times $T_R \lesssim 10^{-4}$ s, such that the corresponding $q^\dagger$ values are higher than the range of q investigated by QELS (10^4 to 3.6×10^5 cm^{-1} (eq 20)).

For instance, let us consider a sample of $M_w = 4.22 \times 10^5$, $c = 7.37 \times 10^{-2}$ g/cm^3, and $T_R \approx 6 \times 10^{-5}$ s ($q^\dagger \approx 4 \times 10^5$ cm^{-1}). At a momentum transfer $q = 3.69 \times 10^4$ cm^{-1}, the decay time τ_T of the correlation function of the photopulses reaches a constant value with the iterative procedure (see Section II.2) and is independent of the time window T of the correlator: for $\tau_T < T \lesssim 6\tau_T$, $\tau_T = (6.81 \pm 0.17) \times 10^{-3}$ s. The variance V_T presents a minimum value of 3×10^{-3} and the quality factor a maximum value of 0.7 ($100Q/V_{T,max} = 2.3$). Using homodyne detection, we find similar behaviors, but the decay time is equal to $\tau_T/2$. These behaviors are characteristic of a concentration correlation function which is well described by a single-exponential function. The inverse of the decay time τ_T is proportional to q^2 (see Figure 2). Those two experimental observations are in agreement with the predictions of Section III.1. Thus, we can identify τ_T with τ_{Lc} (eq 28) and $1/\tau_{Lc}q^2$ with the osmotic diffusion coefficient D_c. In Figure 3, we report values of D_c obtained by QELS with samples of different molecular weights and concentrations and D_c values obtained by classical gradient diffusion (CGD).[19] Within 10%, both measurements are in agreement. For example, by QELS $M_w = 4.22 \times 10^5$, $c = 7.27 \times 10^{-2}$ g/cm^3, and $D_c = 9.5 \times 10^{-8}$ cm^2/s, and by CGD $M_w = 8.6 \times 10^5$, $c = 7.66 \times 10^{-2}$ g/cm^3, and $D_c = 9.12 \times 10^{-8}$ cm^2/s.

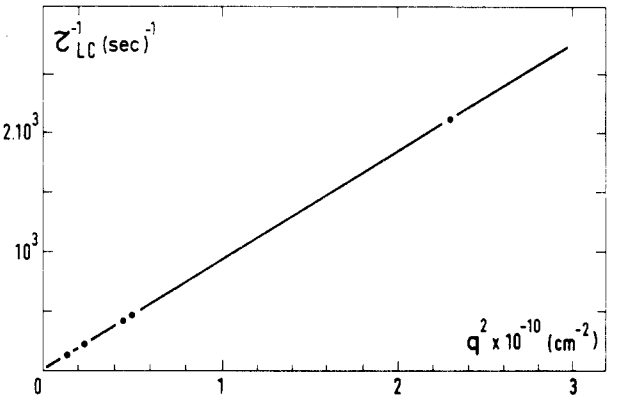

Figure 2. Example of the variation of the inverse of the decay time as a function of the squared momentum transfer in the liquid regime ($100Q_T/V_T$ maximum values are larger than 1). The sample characteristics are $M_w = 4.22 \times 10^5$ and $c = 7.37 \times 10^{-2}$ g/cm^3.

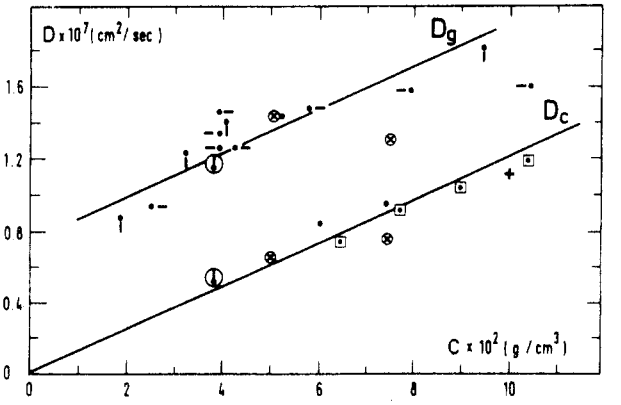

Figure 3. Linear plot of the diffusion coefficients as a function of concentration. The full lines D_c and D_g represent the behaviors of the diffusion coefficients in the liquid (L) and gel (G) regimes of Figure 1. The symbols inside circles are obtained in the transition regime from L to G. For the meaning of the symbols, see Table I. (+) ($M_w = 3.9 \times 10^5$) and (□) ($M_w = 8.6 \times 10^5$) correspond to the diffusion coefficient measured by CGD.[19]

D_c is independent of the molecular weight and can be considered as proportional to the concentration for $c \le 8 \times 10^{-2}$ g/cm^3

$$D_c \text{ (cm}^2 \text{ s}^{-1}) = (1.25 \pm 0.10) \times 10^{-6} c \qquad (34)$$

This variation is represented by the straight line (D_c) in Figure 3.[34,35] The concentration and molecular weight dependence of D_c are in agreement with predictions of section I (eq 6, 7, and 11).

The concentration dependence of D_c is in agreement with intensity light scattering and sedimentation experiments which measure the osmotic compressibility $c(\partial c/\partial \Pi)$ and the effective mobility per monomer μ, respectively. Following section I (see eq 7 and 11) these different

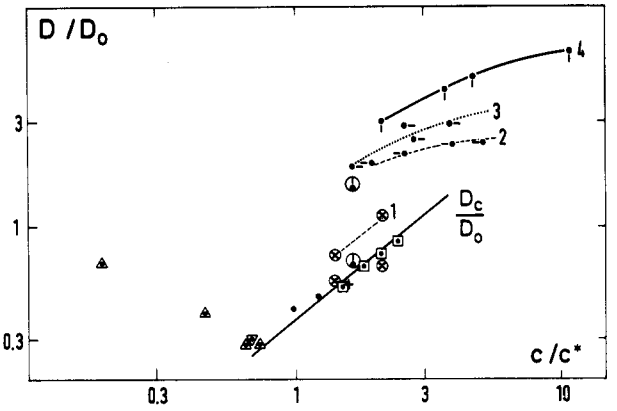

Figure 4. Log–log plot of the variation of the reduced variable D/D_0 as a function of c/c^*, where D_0 is the diffusion coefficient of a single chain. Triangles are values obtained from ref 36: (△) $M_w = 1.3 \times 10^6$; (▽) $M_w = 2 \times 10^6$. The other points have been obtained by using D_0 (cm²/s) $= 1.3 \times 10^{-4}/M_w^{1/2.37}$. For the meaning of the other symbols, see Figure 3. The straight solid line represents $D_c/D_0 \simeq c/c^*$ and the lines 1, 2, 3, and 4 qualitatively represent the variations of D_g/D_0.

quantities are related to each other by the general relation $D_c = \mu(\partial\Pi/\partial c)$. In fact, in a sedimentation experiment, the quantity measured is a sedimentation coefficient s, which is related to μ by $s = (1 - \bar{v}\rho)\mu$. $\bar{v}$ is the partial specific volume of the polystyrene (=0.92 cm³/g) and ρ is the density of the solution (=0.764 g/cm³ at 35 °C). So we have

$$D_c = \frac{s}{(1 - \bar{v}\rho)} \frac{\partial\Pi}{\partial c} \tag{35}$$

Using expression 35 and the experimental results

$$s \text{ (S)} = 1.15 \times 10^{-14} c^{-0.96\pm0.04} \quad \text{(ref 7)}$$

$$\partial\Pi/\partial c \text{ ((dyn cm)/g)} = (2.93 \pm 0.14) \times 10^7 c^2 \quad \text{(ref 4)}$$

we find that

$$D_c = 1.13 \times 10^{-6} c^{1.04} \tag{36}$$

Comparison of expressions 36 and 34 shows that the general relation $D = \mu(\partial\Pi/\partial c)$ is fully respected experimentally. As has been predicted in section I (see eq 13)

$$D_c = k_B T_e / 6\pi\eta_0 \xi_H$$

where ξ_H is the hydrodynamic screening length. The concentration dependence of D_c leads to

$$\xi_H \text{ (cm)} = 2.3 \times 10^{-7}/c$$

Thus in agreement with theory[22] and previous experimental results,[7,19] both lengths ξ_H and ξ are proportional.

Following scaling laws,[24] one must have

$$\xi_H = R_H f(c/c^*)$$

where R_H is the hydrodynamic radius of an isolated polymer chain. This law can be checked by examining the variation of the ratio D_c/D_0 ($D_0 = k_B T_e/6\pi\eta_0 R_H$) as a function of the reduced concentration c/c^*. In Figure 4 we see that the experimental points lie on a single curve whatever the molecular weight and the concentration.

Since c/c^* is a reduced variable of $(Nm/k_B T_e)(\partial\Pi/\partial c)$ and of D_c/D_0, in Θ semidilute solutions, the hydrodynamic and thermodynamic properties can be described with one characteristic length, which is the correlation length ξ of the concentration fluctuations.

b. Gel Regime ($q > q^\dagger$, Region G of Figure 1). Here we present the results obtained from experiments done on samples having long viscoelastic relaxation times ($T_R >$ 20 ms), such that the corresponding $q^\dagger$ values are lower than the range of q investigated by QELS (see eq 20).

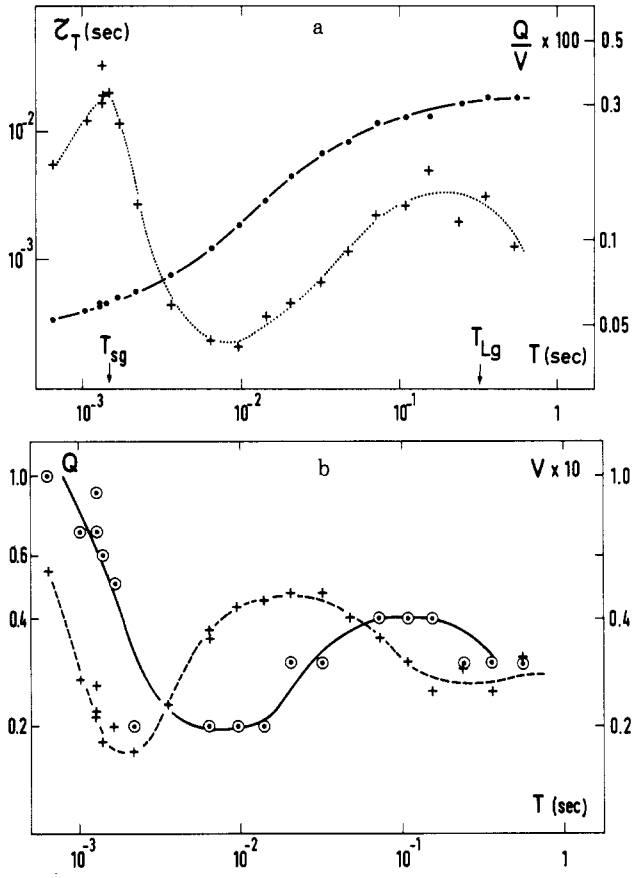

Figure 5. (a) Variation of the decay time τ_T (●) and of $100Q_T/V_T$ (+) as a function of the correlator time window T where the correlation function is analyzed. (b) Variation of the quality factor Q_T (○) and of the relative standard deviation V_T (+) as a function of T. The lines are guides for the eye and the representations are log–log scales.

Let us consider the case of a polymer solution with $M_w = 2.89 \times 10^6$, $c = 3.79 \times 10^{-2}$ g/cm³, and $T_R \approx 1.3 \times 10^{-2}$ s ($q^\dagger \approx 4 \times 10^4$ cm⁻¹). At a $q = 1.448 \times 10^5$ cm⁻¹, the behaviors of the decay time τ_T, the variance V_T, and the quality factor Q_T as a function of the correlator time window T are given in Figure 5a,b. It turns out that τ_T increases continuously with T, but the variation of τ_T with T is weak for $T = T_{Sg}$ and reaches a constant value for $T = T_{Lg}$ (see Figure 5a). At short time (see Figure 5b), T_{Sg} corresponds to a minimum of V_T (1.6×10^{-2}); at long time, T_{Lg} corresponds to a flat minimum of V_T (3×10^{-2}). We determine two decay times, a shortest time τ_{Sg} and a longest time τ_{Lg}, which correspond to maximum values of Q_T/V_T occurring at T_{Sg} and T_{Lg}, respectively (see Figure 5a).

From the signal to baseline ratio R_T (defined in eq 22) determined for $\tau_T = \tau_{Sg}$ and $\tau_T = \tau_{Lg}$, we have access, but with a very poor precision (50%), to the relative amplitude of the slowest to the fastest component (A_L/A_S).

In this section we report the experimental variation of τ_{Sg} and τ_{Lg} as a function of the transfer vector q, only if $\tau_{Lg}/\tau_{Sg} \gtrsim 10^2$.

From Figure 6 one can see that the q dependences proposed for τ_{Sg} and τ_{Lg} (see Table II) are verified experimentally: τ_{Sg} is proportional to q^2 and τ_{Lg} is independent of q. The experimental precision is 10% and 20%, respectively.

The diffusion coefficient D_g [$D_g = 1/(\tau_{Sg}q^2)$] is concentration dependent (see Figure 3) and independent of the molecular weight, in agreement with theoretical predictions

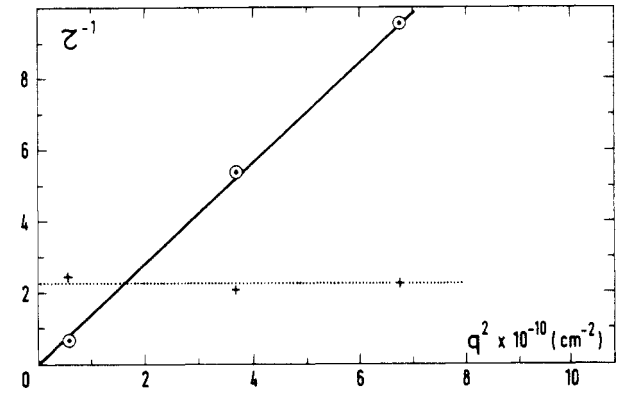

Figure 6. Example of the inverse of decay times as a function of the squared momentum transfer in the gel regime (region G in Figure 1): (○) shortest time τ_{Sg} (ms); (+) longest time τ_{Lg} (s). The sample characteristics are $M_w = 6.77 \times 10^6$ and $c = 3.88 \times 10^{-2}$ g/cm^3.

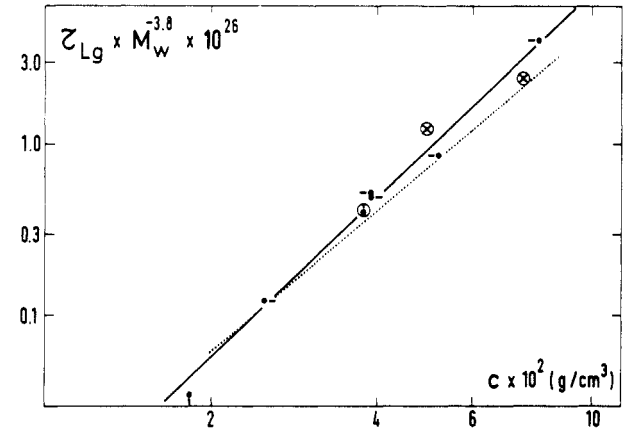

Figure 7. Variation as a function of the concentration of the longest decay time τ_{Lg} (s) divided by the molecular weight dependence ($M_w^{3.8}$). The solid line represents the concentration dependence of τ_{Lg} (see eq 37). For comparison we report (dotted line) the concentration dependence of $T_R/M_w^{3.8}$. T_R is the shear viscoelastic relaxation time measured with the sphere magnetorheometer[10] (for the meaning of the symbols, see Table I).

(eq 6, 7, 9, and 12). For example, at $c = 3.88 \times 10^{-2}$ g/cm^3, D_g is equal to 1.45×10^{-7} and 1.30×10^{-7} cm^2/s for molecular weights of 6.77×10^6 and 3.84×10^6, respectively.

The decay time τ_{Lg}, which corresponds to a structural relaxation, varies strongly with the molecular weight. For instance, at a given concentration $c = 3.88 \times 10^{-2}$ g/cm^3, τ_{Lg} is equal to 0.44 s and to 0.054 s for molecular weights of 6.77×10^6 and 3.84×10^6, respectively. This decay time must have the same molecular weight dependence as the shear viscoelastic relaxation time T_R which was measured using the magnetic sphere rheometer[10,38]: $T_R \sim M_w^{3.8}$. In Figure 7, we see that the quantity $\tau_{Lg}/M_w^{3.8}$ no longer depends on the molecular weight and has the following concentration dependence:

$$\tau_{Lg}\ (\text{s})/M_w^{3.8} = 9.2 \times 10^{-23} c^{3.07\pm0.15} \qquad (37)$$

This experimental result will be discussed in section V.

In Figure 8 are plotted as a function of concentration the relative increment of the diffusion coefficients $D_g/D_c - 1$ and the relative amplitude of A_L/A_S. Within experimental precision, these two quantities are proportional; they decrease as c increases.

This experimental result and the fact that the total intensity scattered is molecular weight independent[4] mean that the amplitude of each component of the dynamical structure factor $S(q,t)$ is molecular weight independent.

The fact that A_L/A_S is smaller than $D_g/D_c - 1$ means that $S(q,t)$ is a multiexponential (>2) function. This is

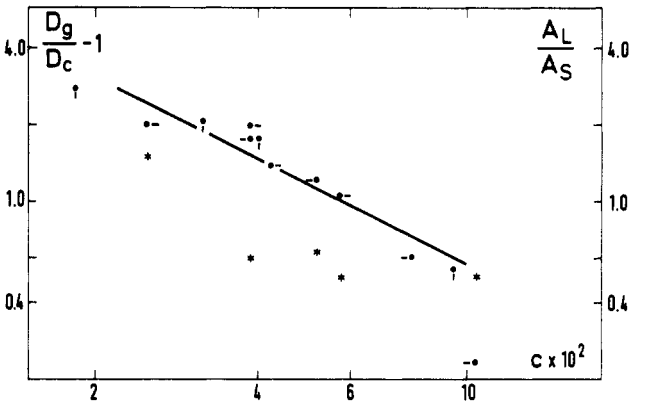

Figure 8. Log–log plots of the relative contribution of the longest to the shortest components (A_L/A_S) (*) and the relative variation of the diffusion coefficients in the liquid and gel regimes ($D_g/D_c - 1$) as functions of concentration. For the meaning of the symbols, see Table I; the straight line corresponds to eq 38.

consistent with the direct observation: τ_T is a continuous increasing function of T (see Figure 5a). The departure of $S(q,t)$ from the predicted two-exponential function (see eq 31) may be due to the distribution of viscoelastic relaxation times:[39] the frequency dependence of the longitudinal elastic modulus does not have the simple form proposed in eq 8. The experimental treatment used allows us to have access only to the shortest and to the longest component of $S(q,t)$.

The relation between the amplitudes of the two components and the diffusion coefficients, $A_L/A_S \approx D_g/D_c - 1$, explains why the slow components are undetectable by QELS in a good solvent system, where it has been found $D_g/D_c \approx 1.1$.[15,18] Moreover, for a given concentration, when the temperature is increased (i.e., when the solution goes from the Θ to the good solvent regime), the amplitude of the short component becomes more and more dominant. For instance, for a sample with $M_w = 6.77 \times 10^6$ and $c = 3.88 \times 10^{-2}$ g/cm^3 the ratio A_S/A_L is of the order of 1.6 at the Θ temperature (35 °C) and greater than 5 above T_e = 50 °C. In a good solvent semidilute solution (polystyrene–benzene[15] or polystyrene–cyclohexane at high temperature) the dynamical structure factor $S(q,t)$ is a single-exponential function. Besides, when the temperature is increased, the gel and osmotic diffusion coefficients increase faster than the inverse of the solvent viscosity (this conforms our previous result[34]).

Let us return to Figure 8 and analyze the concentration dependence of $D_g/D_c - 1$. Experimentally we find that

$$D_g/D_c - 1 = 5.22 \times 10^{-2} c^{-1.04\pm0.2} \qquad (38)$$

Following eq 30, this quantity is equal to M_g/K. From intensity light scattering measurements[4] we have determined

$$K\ (\text{dyn/cm}^2) = (2.93 \pm 0.14) \times 10^7 c^3 \qquad (39)$$

So our measurements lead to a longitudinal elastic modulus that has the following dependence:

$$M_g\ (\text{dyn/cm}^2) = 1.53 \times 10^6 c^{1.96} \qquad (40)$$

Although M_g and K do not have the same concentration dependence, they are of the same order of magnitude (for $c = 5 \times 10^{-2}$ g/cm^3, $M_g/K = 1$).

The mean quadratic distance ξ_2^2 between two contact points is linked to the longitudinal elastic modulus by $\xi_2^2 \sim c/M_g$. Thus we obtain

$$\xi_2^2 \sim c^{-0.96}$$

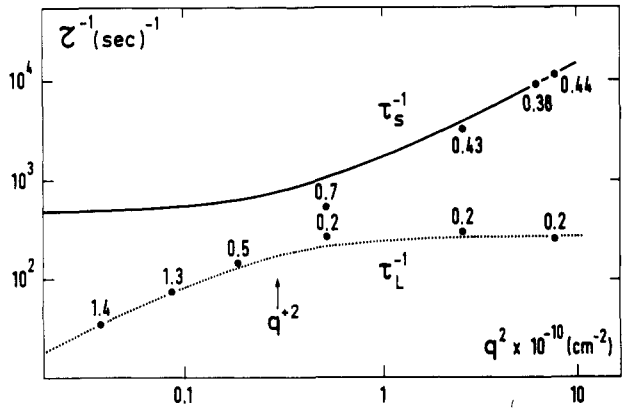

Figure 9. Log–log plots of variations of the inverse of the decay times in the transition from L to G regimes as a function of q^2. Dotted and full lines correspond to the theoretical behaviors of the longest and shortest decay times, respectively (see (A.7)). The numerical values attached to the experimental points are $100Q_T/V_T$ maximum values. Sample characteristics are $M_w = 1.26 \times 10^6$ and $c = 7.42 \times 10^{-2}$ g/cm^3.

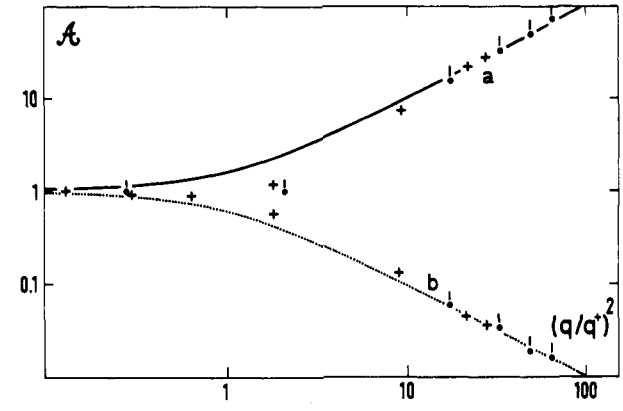

Figure 10. Log–log plots of the reduced quantity $\mathcal{A}$ equal to $(D_g/D_g)(\tau_{Lg}/\tau_S) = \tau_S^{-1}/\tau_R^{-1}$ or to $\tau_L^{-1}/(D_c q^2)$ as a function of $q/q^\dagger$ ($q^{\dagger 2} = 1/(D_c\tau_{Lg})$). Curves a and b correspond to the theoretical behaviors of τ_S^{-1}/τ_R^{-1} and of $\tau_L^{-1}/(D_c q^2)$, respectively (see eq 26c). (+) $M_w = 1.26 \times 10^6$, $c = 7.42 \times 10^{-2}$ g/cm^3; (●, pip up) $M_w = 2.89 \times 10^6$, $c = 3.79 \times 10^{-2}$ g/cm^3.

This concentration dependence is in agreement with eq 3, and one can conclude that the longitudinal elastic modulus is sensitive to the binary contact points, in agreement with theoretical predictions of ref 22 and 23.

In Figure 4 we can see that the relative concentration c/c^* is not a reduced variable of D_g/D_0, where D_0 is the diffusion coefficient of a single chain. Since the gel diffusion coefficient is sensitive to two lengths ξ (via K) and ξ_2 (via M_g), this means that in contrast to ξ/R, which is a function of c/c^*, ξ_2/R is not a function of c/c^* ($\xi_2 \simeq [Ra(c^*/c)]^{1/2}$, where a is the statistical length).

Until now we have analyzed the experimental results obtained either in the region L of Figure 1 or in the region G of Figure 1. We will present now the transition from the liquid regime (L) to the gel regime (G) observed by increasing the transfer vector q.

c. Transition from the Liquid Regime to the Gel Regime. Here we present the results obtained from experiments done on samples having an intermediate viscoelastic relaxation time ($T_R \approx 10^{-3}$ s) such that the corresponding $q^\dagger$ values are in the q range investigated by QELS (see eq 20).

A characteristic behavior of the decay times of the correlation function vs. the squared momentum transfer is given in Figure 9 ($M_w = 1.26 \times 10^6$, $c = 7.42 \times 10^{-2}$ g/cm^3, and $q^\dagger = 5.4 \times 10^4$ cm^{-1}).

For $q < q^\dagger$, the correlation function can be described by a single-exponential function. As the q vector is lowered, the quantity $(Q/V)_{max}$ increases (see Figure 9); thus the profile becomes more and more exponential and the ratio $1/(\tau_L q^2)$ becomes a constant equal to 9.1×10^{-8} cm^2/s. This diffusion coefficient value (D_c) is in agreement with results obtained in the liquid regime (Figure 3 the points corresponding to these experimental results are placed inside circles).

For $q > q^\dagger$, we recover the profile of the correlation function described in the gel regime. At large values of $q/q^\dagger$ ($q/q^\dagger > 2.8$), the decay time τ_L of the slow component becomes independent of q ($\tau_L = \tau_{Lg} = 3.8 \times 10^{-3}$ s) and the decay time τ_S of the fast component shows a q^{-2} dependence ($\tau_S = \tau_{Sg} = 1/(D_g q^2)$ with $D_g = 1.53 \times 10^{-7}$ cm^2/s). The diffusion coefficient D_g and the decay time τ_{Lg} obtained here agree with the results found in the gel regime (see Figures 3 and 7, points inside circles).

The lines in Figure 9 correspond to the theoretical behavior proposed (appendix, eq A.7) in which we have used $\tau_R = (D_c/D_g)\tau_{Lg}$ and inserted the experimental values of D_g, D_c and τ_{Lg}. The experimental values of τ_L^{-1} and τ_S^{-1} follow approximatively the theoretical curves, but the transitions between the two regimes are more abrupt than those predicted. This can be due to the fact that for $q \approx q^\dagger$, the theoretical amplitudes and the decay times of the shortest and longest component are of the same order of magnitude so the values of τ_S and τ_L measured are correlated.

In Figure 10, we plot τ_S^{-1}/τ_R^{-1} and $\tau_L^{-1}/(D_c q^2)$ vs. $q/q^\dagger$ for the experimental values obtained with two samples: $M_w = 1.26 \times 10^6$, $c = 7.42 \times 10^{-2}$ g/cm^3, and $\tau_{Lg} = 3.8 \times 10^{-3}$ s; $M_w = 2.89 \times 10^6$, $c = 3.79 \times 10^{-2}$ g/cm^3, and $\tau_{Lg} = 1.31 \times 10^{-2}$ s.

In the regime $(q/q^\dagger)^2 > 10$, the experimental values are on the same master curve whatever the molecular weight and the concentration of the samples, in agreement with the proposed law (26c).

Thus $q^\dagger$, which is strongly molecular weight dependent, is, as has been proposed (see section III), a momentum transfer that separates two dynamical regimes: the liquid and the gel regimes.

2. Internal Motion (Region I of Figure 1). Since the correlation length is inversely proportional to the concentration, in order to observe internal motion with QELS we have to use low-concentration samples: $c_1 = 1.82 \times 10^{-2}$ g/cm^3, $M_w = 20.6 \times 10^6$; $c_2 = 2.48 \times 10^{-2}$ g/cm^3, $M_w = 6.77 \times 10^6$.

With such samples, and by increasing the q vector, we can observe either the gel regime or the internal motion regime and thus go from the G region to the I region of Figure 1.

In region I, the pattern of τ_T vs. the correlator time window T is similar to that given in Figure 5 but the $(Q/V)_{max}$ values corresponding to the shortest decay time τ_{Sg} are lower than the values obtained in the gel regime. This experimental observation is obvious because $q^\dagger$ is always smaller than ξ^{-1}.

We focus our attention on the q dependence of the gel diffusion coefficient and plot in Figure 11 $\tau_{Sg}^{-1}/(D_g q^2)$ as a function of $q\xi$. It appears that at $q\xi < 1/3$, $\tau_{Sg}^{-1}/(D_g q^2) = 1$ and is independent of q, and at $q\xi > 1/3$, $\tau_{Sg}^{-1}/(D_g q^2)$ is an increasing function of q and concentration dependent in this representation.

Thus QELS probes diffusive processes at $q\xi < 1/3$, and internal motion at $q\xi > 1/3$, but $q\xi$ is not the reduced variable of $\tau_{Sg}^{-1}/(D_g q^2)$.

This has to be compared to the dilute Θ solution, where it was found[40,41] that qR_g is a reduced variable of $\tau^{-1}/(D_0 q^2)$,

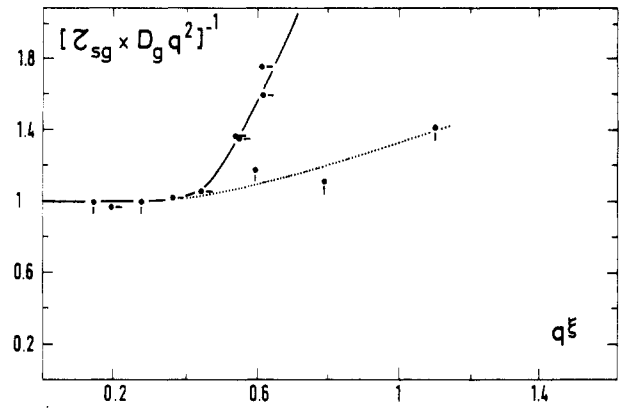

Figure 11. Variation of the reduced effective diffusion coefficient, $1/(\tau_{Sg}D_gq^2)$, as a function of the dimensionless quantity $q\xi$. Solid lines are only guides for the eye. (●, pip down) $M_w = 20.6 \times 10^6$, $c_1 = 1.82 \times 10^{-2}$ g/cm^3; (●, pip right) $M_w = 6.77 \times 10^6$, $c_2 = 2.48 \times 10^{-2}$ g/cm^3.

which departs from unity at $qR_g \approx 1$.

Now let us compare the experimental results of Figure 11 to the theoretical expression (eq 32)

$$\tau_{Sg}^{-1}/(D_gq^2) = F(q\xi)(M_g/K + 1 + q^2\xi^2)/(M_g/K + 1)$$

If, as suggested by this relation, the concentration dependence of $\tau_{Sg}^{-1}/(D_gq^2)$ vs. $q\xi$ comes through the moduli term only, we can explain qualitatively, but not quantitatively, the experimental results. At a given value of $q\xi$, the higher the value of M_g/K (the lower the concentration), the lower is the value of $\tau_{Sg}^{-1}/(D_gq^2)$. But taking for M_g/K the macroscopic quantities (see eq 30 and 38), we find, using expression 32

$$\frac{[\tau_{Sg}^{-1}/(D_gq^2)]_{c_2}}{[\tau_{Sg}^{-1}/(D_gq^2)]_{c_1}} = 1.02 \qquad \text{at } q\xi = 0.6$$

instead of the value 1.4 found experimentally.

This can be due to the fit of the dynamical structure factor, which could be incorrect for $q\xi > {}^1/_3$, to the experimental evidence that the crossover between a diffusive process and internal motion appears at $q\xi = {}^1/_3$ instead of $q\xi = 1$ (found with relation 32), or to the assumption that M_g is a constant independent of q.

It would be interesting to study the internal motion of a semidilute solution over a wider range of q. This can be realized either by increasing ξ and thus the molecular weight in order to fulfil the semidilute condition (see relation 19) or by decreasing q and thus using quasi-elastic neutron scattering.

In any case, the fact that $q\xi$ is not a reduced variable of $\tau_{Sg}^{-1}/(D_gq^2)$ is further evidence that longitudinal elastic and osmotic bulk moduli are of the same order of magnitude but are sensitive to two different lengths in the Θ condition.

V. Comparison between Quasi-Elastic Light Scattering and Viscoelastic Measurements

From viscoelastic measurements,[10] we know that the shear elastic modulus G_g is sensitive to the binary contact point and is equal to

$$G_g \text{ (dyn/cm}^2) = 1.34 \times 10^6 c^{2.5\pm0.2} \qquad (41)$$

From QELS and intensity light scattering experiments we have deduced the longitudinal modulus (eq 40): $M_g = 1.53 \times 10^6 c^{1.96}$ dyn/cm^2.

Within the experimental precision the two quantities are proportional:

$$M_g = 6.5G_g \qquad (42)$$

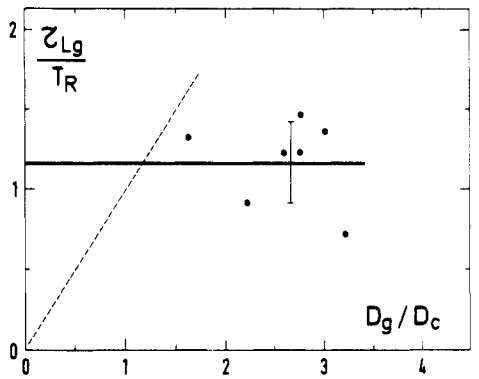

Figure 12. Ratio of the longest decay time τ_{Lg} to the shear viscoelastic time T_R as a function of the ratio of the gel to the osmotic diffusion coefficient. Solid line represents the mean value of τ_{Lg}/T_R. Dotted line corresponds to eq 30 when τ_R is identified to T_R.

6.5 corresponds to the mean value calculated in the concentration range 2×10^{-2} to 8×10^{-2} g/cm^3. Following viscoelastic theory of an isotropic medium,[42] we have

$$M_g = K_g + {}^4/_3G_g \qquad (43)$$

Comparing (42) and (43) we find

$$K_g = 5.2G_g \qquad (44)$$

We must note that this elastic bulk modulus K_g does not correspond to that of an incompressible medium polymer plus solvent ($K_{bulk} \approx 10^4 G_{bulk}$[39]) but to that of a medium in which the solvent is allowed to be displaced when a high-frequency ($\omega\tau_R \gg 1$) compressional force is applied to the polymer.

If one assumes that $M_g = 6.5G_g$ whatever the quality of the solvent, we can understand the QELS results in a good solvent. We know that

$$A_L/A_S \approx D_g/D_c - 1 = M_g/K \approx 6.5(G_g/K)$$

Actually, on increasing the quality of solvent, G_g decreases slightly while K increases strongly; typically at $c = 4 \times 10^{-2}$ g/cm^3 we have $G_{gGS} \approx 0.9G_{g\Theta}$ and $K_{GS} \approx 32K_\Theta$ (where GS means the good solvent polystyrene–benzene system).[4,9,10] Thus in good solvent $D_g = 1.04D_c$ and the longest decay time is undetectable (in agreement with experimental results).

At this stage it is interesting to compare the decay time τ_R associated with the longitudinal structural relaxation and the time T_R obtained from shear viscoelastic measurements on the same samples.[10] In Figure 12 we have plotted τ_{Lg}/T_R against D_g/D_c; obviously the conclusion is that τ_{Lg} is equal to T_R:$\tau_{Lg}/T_R = 1.17 \pm 0.20$.[43] This result can also be observed in Figure 7, where the dotted line corresponds to T_R values measured with the magnetic sphere rheometer;[10] the full line corresponds to τ_{Lg} measured in this experiment.

Using the definition of $\tau_{Lg} = (D_g/D_c)\tau_R$ (see eq 30), we have

$$\tau_{Lg} = T_R = [1 + (M_g/K)]\tau_R \qquad (45)$$

The longitudinal relaxation τ_R must be smaller than the shear relaxation time T_R, and the two times have the same molecular weight dependence but must not have the same concentration dependence. In ref 10, it has been shown that the shear reduced time T_R/T_1 (where T_1 is the first mode of a single chain) is not just a function of c/c^*; the same conclusion can be drawn for the longitudinal reduced time τ_R/T_1. The friction involved in the displacement of one chain is not purely hydrodynamic since hydrodynamic

and thermodynamic quantities follow scaling law. We must note that the situation is different in a good solvent where T_R/T_1 follows a scaling law,[9] and $\tau_R/T_1 = 1$ because $M_g/K \approx 10^{-2}$.

Conclusion

The quasi-elastic light scattering results presented here are different from those reported by other groups[44-49] but are in perfect agreement with measurements performed with different techniques.

Experiments performed on homogeneous semidilute Θ solutions (10^{-1} g/cm$^3 > c > c^*$) show that many dynamical regimes exist, in agreement with theoretical predictions.[22,23]

At a time scale where the Θ semidilute solution behaves like a viscous fluid (i.e., the shear viscosity is Newtonian), the time dependence of the dynamical structure factor is an exponential function and the inverse of the decay time is proportional to q^2: $1/\tau_{Lc} = D_c q^2$. The diffusion coefficient D_c, independent of the molecular weight, increases linearly with the monomer concentration: D_c (cm^2/s) = $1.25 \times 10^{-6}c$. The comparison between the D_c values and measurements of the effective mobility μ, obtained by sedimentation,[17] and of the osmotic compressibility $\partial c/\partial \Pi$, obtained by intensity light scattering measurements,[4] shows that the diffusion coefficient $D_c = \mu(\partial \Pi/\partial c)$ is linked to the osmotic force and to the hydrodynamic interactions. The osmotic diffusion D_c is inversely proportional to the correlation length ($\xi \sim c^{-1}$) of the concentration fluctuations; the hydrodynamic and thermodynamic properties can be described with only one characteristic length ξ. In the liquid regime the relaxation of the concentration fluctuations is controlled by the motion of the solvent through the polymer.

At a time scale where the Θ semidilute solution behaves like a gel (i.e., the solution has a finite elastic modulus), the time dependence of the dynamical structure factor is multiexponential (>2). At the shortest times we can define a characteristic decay time τ_{Sg}, which is proportional to q^{-2}, and determine a gel diffusion coefficient D_g, which is only concentration dependent. At the longest times we can define a characteristic time τ_{Lg}, which is independent of q and equal to the shear relaxation time obtained from mechanical measurements. The longitudinal relaxation time τ_{Lg} is strongly concentration and molecular weight dependent: $\tau_{Lg} \sim M_w^{3.8}c^3$. In the gel regime, the relaxation of the fluctuation concentrations is mainly governed by two processes: at the shortest times by the diffusion of the solvent through the transient gel and at the longest times by the structural relaxation of the transient gel.

At a temperature higher than Θ, in the good solvent regime, we find that whatever the time scale the profile of the dynamical structure factor is an exponential function, in agreement with our previous results in polystyrene–benzene.[15]

If the concentration dependence of the characteristic time τ_{Lg} may be understood in terms of hydrodynamic friction, the high value of the molecular weight exponent (3.8) indicates that for longitudinal as well as for shear relaxation times the friction involved in the disentanglement of a chain under Θ conditions is not purely hydrodynamic.

Comparing the gel to the osmotic diffusion coefficient, we find that the longitudinal elastic modulus M_g and the osmotic bulk modulus K are of the same order of magnitude but that their concentration dependences are different: $M_g = 1.53 \times 10^6 c^{1.96}$ and $K = 2.93 \times 10^7 c^3$.[4] From this concentration dependence we conclude that the elastic modulus M_g is sensitive to the mean distance ξ_2 between binary contact points ($M_g \sim k_B T_e c/\xi_2^2$) with $\xi_2^2 \sim c^{-1}$), while the thermodynamic modulus K is sensitive to ξ ($K \simeq k_B T_e/\xi^3$).

For the first time we have observed the transient gel by quasi-elastic light scattering. We have also observed a difference between the correlation length of concentration fluctuations and the mesh size of the transient gel in semidilute Θ solutions.

Acknowledgment. We thank P.-G. de Gennes, F. Brochard, and J. D. Ferry for stimulating discussions and J. Ròots, B. Nyström, J. P. Munch, and S. Candau for kindly communicating the numerical values of ref 19 and 36.

Appendix. Dynamical Structure Factor

Quasi-elastic light scattering allows the dynamical structure factor $S(q,t)$ to be determined[31]

$$S(q,t) = \langle \delta c_q(t) \delta c_q^\dagger(0) \rangle / V \tag{A.1}$$

V is the scattering volume and $\delta c_q(t)$ is the space Fourier transform of the concentration fluctuation

$$\delta c_q(t) = \int_V \delta c(\mathbf{r},t) e^{-i\mathbf{q}\cdot\mathbf{r}}\, d\mathbf{r} \tag{A.2}$$

In order to calculate the time dependence of $S(q,t)$, it is convenient to know the longitudinal displacement u of the polymer system induced by a perturbative periodic force of frequency ω and wave vector q: $f_0 e^{i(qx-\omega t)}$. Let us write

$$u(q,\omega) = \chi(q,\omega) f_0 e^{i(qx-\omega t)} \tag{A.3}$$

The dynamical structure factor $S(q,t)$ is related to the response function $\chi(q,\omega)$ by the relation[22,23,50]

$$S(q,\omega) = -c^2 q^2 \frac{k_B T_e}{\pi} \int_{-\infty}^{+\infty} \omega^{-1} \chi''(q,\omega) e^{i\omega t}\, d\omega \tag{A.4}$$

where $\chi''(q,\omega)$ is the imaginary part of $\chi(q,\omega)$.

In the presence of the external force $f_0 e^{i(qx-\omega t)}$ the equation of motion (eq 5) becomes

$$i\omega c u/\mu + K q^2 u + M(\omega) q^2 u = f_0 e^{i(qx-\omega t)} \tag{A.5}$$

From eq A.3 and A.5 and the expressions of $M(\omega)$, D_c, and D_g (see eq 8, 11, and 12), it follows that

$$\chi(q,\omega) = -\mu(1 + i\omega\tau_R)/c\tau_R D'(q,\omega)$$

$$D'(q,\omega) = \omega^2 - i\omega(\tau_R^{-1} + D_g q^2) - \tau_R^{-1} D_c q^2 \tag{A.6}$$

If $D_g > D_c$, the roots of $D'(q,\omega)$ are two purely imaginary numbers

$$\omega_1 = i/\tau_S \quad \text{and} \quad \omega_2 = i/\tau_L$$

$$\tau_S^{-1} = \frac{1}{2}\left[1/\tau_R + D_g q^2 + \left[\left(\frac{1}{\tau_R} + D_g q^2\right)^2 - 4D_c q^2/\tau_R\right]^{1/2}\right]$$

$$\tau_L^{-1} = \frac{1}{2}\left[1/\tau_R + D_g q^2 - \left[\left(\frac{1}{\tau_R} + D_g q^2\right)^2 - 4D_c q^2/\tau_R\right]^{1/2}\right] \tag{A.7}$$

with $\tau_S \le \tau_R \le \tau_L$.

If q^{-1} is larger than the correlation length ξ, D_c and D_g are q independent. Using in (A.7) $q^\dagger = (1/\tau_R D_G)^{1/2}$, the momentum transfer that separates the liquid and the gel regime, we obtain for τ_S and τ_L the expression (26c).

The fact that the roots of $D'(q,\omega)$ are imaginary numbers implies that $\chi''(q,\omega)$ is the sum of two Lorentzian functions

$$-\chi''(q,\omega)/\omega = 1/Kq^2\left[\frac{\tau_S A_S}{\omega^2\tau_S^2+1}+\frac{\tau_L A_L}{\omega^2\tau_L^2+1}\right] \quad (A.8)$$

where A_S and A_L have the following dependences:

$$A_S = (\tau_R - \tau_S)/(\tau_L - \tau_S)$$
$$A_L = 1 - A_S = (\tau_L - \tau_R)/(\tau_L - \tau_S) \quad (A.9)$$

Following eq A.4, the frequency Fourier transform of eq A.8 allows us to obtain the dynamical structure factor

$$S(q,t) = k_B T_e \frac{c^2}{K}\tilde{S}(q,t)$$
$$\tilde{S}(q,t) = [A_S e^{-|t|/\tau_S} + A_L e^{-|t|/\tau_L}] \quad (A.10)$$

Registry No. Polystyrene, 9003-53-6; cyclohexane, 110-82-7.

References and Notes

(1) Daoud, M.; Cotton, J. P.; Farnoux, B.; Jannink, G.; Sarma, G.; Benoit, H.; Duplessix, R.; Picot, C.; de Gennes, P.-G. *Macromolecules* **1975**, *8*, 804.
(2) Cotton, J. P.; Nierlich, M.; Boue, F.; Daoud, M.; Farnoux, B.; Jannink, G.; Duplessix, R.; Picot, C. *J. Chem. Phys.* **1976**, *65*, 1101.
(3) Amirzadeh, J.; McDonnell, M. E. *Macromolecules* **1982**, *15*, 927.
(4) Stepanek, P.; Perzynski, R.; Delsanti, M.; Adam, M. *Macromolecules* **1984**, *17*, 2340.
(5) Wiltzius, P.; Haller, H. R.; Cannell, D. S.; Schaefer, D. W. *Phys. Rev. Lett.* **1983**, *51*, 118.
(6) Noda, I.; Kato, N.; Kitano, T.; Nagasawa, M. *Macromolecules* **1981**, *14*, 668.
(7) Vidakovic, P.; Allain, C.; Rondelez, F. *J. Phys. (Les Ulis, Fr.)* **1981**, *42*, L323.
(8) Roots, J.; Nyström, B.; Sundelof, L. O.; Porsh, B. *Polymer* **1979**, *20*, 337.
(9) Adam, M.; Delsanti, M. *J. Phys. (Les Ulis, Fr.)* **1983**, *44*, 1185.
(10) Adam, M.; Delsanti, M. *J. Phys. (Les Ulis, Fr.)* **1984**, *45*, 1513.
(11) Leger, L.; Hervet, H.; Rondelez, F. *Macromolecules* **1981**, *14*, 1732.
(12) Wesson, J. A.; Noh, I.; Kitano, T.; Yu, H. *Macromolecules* **1984**, *17*, 782.
(13) Callaghan, P. T.; Pinder, D. N. *Macromolecules* **1981**, *14*, 1334.
(14) von Meerwall, E. D.; Amis, E. J.; Ferry, J. D. *Macromolecules* **1985**, *18*, 260.
(15) Adam, M.; Delsanti, M. *Macromolecules* **1977**, *10*, 1229.
(16) Wiltzius, P.; Haller, H. R.; Cannell, D. S.; Schaefer, D. W. *Phys. Rev. Lett.* **1984**, *53*, 834.
(17) Munch, J. P.; Candau, S.; Herz, J.; Hild, G. *J. Phys. (Les Ulis, Fr.)* **1977**, *38*, 971.
(18) Adam, M.; Delsanti, M.; Pouyet, G. *J. Phys. (Les Ulis, Fr.)* **1979**, *40*, L435.
(19) Roots, J.; Nyström, B. *Macromolecules* **1980**, *13*, 1595.
(20) de Gennes, P.-G. *Macromolecules* **1976**, *9*, 587.
(21) de Gennes, P.-G. *Macromolecules* **1976**, *9*, 594.
(22) Brochard, F.; de Gennes, P.-G. *Macromolecules* **1977**, *10*, 1157.
(23) Brochard, F. *J. Phys. (Les Ulis, Fr.)* **1983**, *44*, 39.
(24) de Gennes, P.-G. "Scaling Concepts in Polymer Physics"; Cornell University Press: Ithaca, NY, 1979.
(25) If A = constant × B and the constant is dimensionless we will write $A \simeq B$. $A \sim B$ means that A is proportional to B. $A \approx B$ means that A is of the order B.
(26) Ferrel, R. A. *Phys. Rev. Lett.* **1970**, *24*, 1169.
(27) He, M.; Kubota, K.; Pope, J.; Chu, B. *Macromolecules* **1982**, *15*, 673.
(28) Adam, M.; Delsanti, M.; Pieranski, P.; Meyer, R. *Rev. Phys. Appl.* **1984**, *19*, 253.
(29) Decker, D. Thesis, Strasbourg, 1968.
(30) Strazielle, C.; Benoit, H. *Macromolecules* **1975**, *8*, 203.
(31) Cummins, H. Z.; Pike, E. R. "Photon Correlation and Light Beating Spectroscopy"; Plenum Press: New York, 1974.
(32) Mathews, J.; Walker, R. L. "Mathematical Methods of Physics"; W. A. Benjamin: Reading, MA, 1964.
(33) Tournarie, M. *J. Phys. (Les Ulis, Fr.)* **1969**, *30*, 47.
(34) Adam, M.; Delsanti, M. *J. Phys. (Les Ulis, Fr.)* **1980**, *41*, 713.
(35) In ref 34 we reported a QELS experiment on a sample $c = 8.49 \times 10^{-2}$ g/cm^3 whose nominal molecular weight was $M_w = 3.8 \times 10^6$. Following the results obtained in the present paper (see section IV) and the T_R value ≈ 0.4 s estimated from Table I, we expect that, for this sample, we must have access to a gel diffusion coefficient D_g by QELS. In fact, a diffusion coefficient of $(9.85 \pm 0.20) \times 10^{-8}$ cm^2/s was found, which agrees with D_c expression 34. This must be due to the polydispersity of the sample, which reduces the value of the shear viscoelastic relaxation time.
(36) Munch, J. P.; Hild, G.; Candau, S. *Macromolecules* **1983**, *16*, 71.
(37) Schmidt, M.; Burchard, W. *Macromolecules* **1981**, *14*, 210.
(38) We must note that the law $T_R \sim M^{3.8}$ does not agree with the theoretical scaling law $T_R = T_1 (c/c^*)^3$ used in the construction of Figure 1.
(39) Ferry, J. D. "Viscoelastic Properties of Polymers", 3rd ed.; Wiley: New York, 1980.
(40) Han, C. C.; Akcasu, A. Z. *Macromolecules* **1981**, *14*, 1080.
(41) In dilute solution ($c < c^*$), we have $S(q,0) = ck_BT_e/(\partial\Pi/\partial c)(1 + q^2R_g^2/3)$ for $qR_g < 1$. In semidilute solution ($c > c^*$), we have $S(q,0) = ck_BT_e/(\partial\Pi/\partial c)(1 + q^2\xi^2)$.[2,24] At c^* the two structure factors must coincide, so we have $\xi = R/3^{1/2}$.
(42) See, for instance: Landau, L.; Lifschitz, F. "Theory of Elasticity"; Pergamon Press: London, 1970.
(43) Adam, M.; Delsanti, M. *J. Phys. (Les Ulis, Fr.)* **1984**, *45*, L279.
(44) Amis, E. J.; Han, C. C. *Polymer* **1982**, *23*, 1403.
(45) Amis, E. J.; Han, C. C.; Matsushita, Y. *Polymer* **1984**, *25*, 650.
(46) Schaefer, D. W.; Han, C. C. Sandia Report, Apr 1982.
(47) Brown, W.; Johnsen, R. *27th Microsymp. Macromolecules Prague 1984.*
(48) Nose, T.; Chu, B. *Macromolecules* **1979**, *12*, 599, 1122. In this work, the experiments were performed on a 1.7×10^5 molecular weight sample; the semidilute condition ($c^* < c < 10^{-1}$ g/cm^3) is not fulfilled.
(49) Hecht, A. M.; Bohidar, H. B.; Geissler, E. *J. Phys. (Les Ulis, Fr.)* **1984**, *45*, L121. The results obtained in this work are qualitatively in agreement with our results. But the D_c and D_g values differ from ours by a factor of 2. We must note that D_c cannot be measured by QELS with a monodisperse sample of 26×10^6 molecular weight because $q^\dagger$ is too small.
(50) Landau, L.; Lifschitz, F. "Physique Statistique"; Mir: Moscow, 1967.